ORIGINAL ARTICLE

CrossMark

Fibroblast growth factor receptor 1 signaling transcriptionally regulates the axon guidance cue *slit1*

Jung-Lynn Jonathan Yang[1] · Gabriel E. Bertolesi[1] · Carrie L. Hehr[1] · Jillian Johnston[1] · Sarah McFarlane[1]

Abstract

Axons sense molecular cues in their environment to arrive at their post-synaptic targets. While many of the molecular cues have been identified, the mechanisms that regulate their spatiotemporal expression remain elusive. We examined here the transcriptional regulation of the guidance gene *slit1* both in vitro and in vivo by specific fibroblast growth factor receptors (Fgfrs). We identified an Fgf-responsive 2.3 kb *slit1* promoter sequence that recapitulates spatiotemporal endogenous expression in the neural tube and eye of *Xenopus* embryos. We found that signaling through Fgfr1 is the main regulator of *slit1* expression both in vitro in A6 kidney epithelial cells, and in the *Xenopus* forebrain, even when other Fgfr subtypes are present in cells. These data argue that a specific signaling pathway downstream of Fgfr1 controls in a cell-autonomous manner *slit1* forebrain expression and are novel in identifying a specific growth factor receptor for in vivo control of the expression of a key embryonic axon guidance cue.

Keywords Axon guidance · Forebrain · Promoter · Retinal ganglion cell · Signal transduction · *Xenopus*

Introduction

The establishment of a functional neural network requires that neurons make proper synaptic connections. Attractive and repulsive guidance cues in the milieu direct growing axons toward their appropriate post-synaptic targets. The molecular identity of these cues has been studied extensively [1–3], and a relatively small number of cues control the connections made by neurons throughout the nervous system. Thus, for an extensive number of specific connections to be made, the expression of individual cues and their receptors needs to be tightly regulated both spatially and temporally. The molecular mechanisms behind the spatiotemporal regulation of these cues during development, however, are poorly understood.

✉ Sarah McFarlane
  smcfarla@ucalgary.ca

1   Department of Cell Biology and Anatomy, Hotchkiss Brain
    Institute, Alberta Children's Hospital Research Institute,
    Cumming School of Medicine, University of Calgary, 3330
    Hospital Dr., NW, Calgary, AB T2N 4N1, Canada

During development, four main families of guidance cues interact with their specific receptors to drive axons to their post-synaptic targets. Netrin, Ephrin, Slit, and Semaphorin ligands bind to receptors DCC/UNC5, Eph, Robo/EVA1C, and Plexins/Neuropilins, respectively [2–4]. Our knowledge of the transcriptional mechanisms that regulate these axon guidance molecules is based mostly on the tumorigenic context, where, for instance, the expression of members of the *SLIT* family (*SLIT1*–3) is downregulated by hypermethylation in human cancers [5–7]. Additionally, the EZH2 polycomb repressive complex binds and inhibits the *SLIT2* promoter in prostate cancer [5, 8, 9].

Within a developmental context, we know more about the regulation of the expression of guidance receptors than guidance ligands, as the receptors are often regulated indirectly as part of the differentiation program of a neuron. For instance, the transcription factor Eve, and other stereotypical repressors such as Nkx6 and Engrailed likely exert indirect regulation of guidance receptor genes by de-repression of yet unknown factor(s) [10]. Further, there are examples of transcription factors binding to the *cis*-regulatory regions of receptor genes. Eve, Dbx1, and Isl2 bind to and exert direct transcriptional control of the axon guidance receptor genes *unc5*, *ROBO3*, and *PLXNA4*, respectively [10–12]. Additionally, COUP-TFII complexes with Sp1 to activate Neuropilin

2 (Nrp2) at specific Sp1 sites of the *Nrp2* locus [13], and Fezf2 binds to the proximal promoter of *Ephb1* [14].

Transcription factors become active downstream of cell extrinsic signaling molecules. However, current knowledge about the regulation of guidance genes in vivo by extrinsic signaling molecules is limited. We do know that hedgehog (Hh) signaling drives netrin1 (*ntn1*) in zebrafish [15] in a manner distinct from the patterning role of Hh signaling to indirectly control guidance genes by regulating cell identity [16, 17], i.e., Hh signaling drives ectopic *ntn1* in determined cells that do not express *ntn1*. Fibroblast growth factor (Fgf) signaling is another example where a canonical morphogen has a non-canonical role in regulating guidance cue expression [18].

In mammals, there are 18 FGFs that bind four transmembrane FGF receptors (FGFR1–4) [19, 20]. Each FGFR has tyrosine kinase domains whose activation evokes intracellular signaling cascades [21]. FGFs initiate *Semaphorin3f* and *EphrinA2/5* expression in the midbrain [22, 23]. They do so, however, as a result of tissue patterning. Thus, it is unclear whether FGF signaling can directly regulate the expression of axon guidance genes, or if FGFs do so as a by-product of altering tissue identity and/or cell proliferation.

In this regard, we found previously that Fgfs positively regulate *slit1* and *sema3a* expression in the *Xenopus* forebrain, independently of a patterning role [18]. Slit1 and Sema3a, in conjunction, repel *Xenopus* optic tract axons out of the mid-diencephalon in the direction of their dorsal midbrain target, the optic tectum. Interestingly, ongoing Fgf signaling is required to maintain the expression of the guidance cues. Fgf8 overexpression expands the *slit1* domain of expression, while *slit1* is rapidly downregulated with pharmacological inhibition of Fgf signaling. Downregulation of *slit1* and *sema3a* together, either directly by mRNA knockdown or indirectly via Fgfr inhibition, results in optic tract axons collecting aberrantly in the mid-diencephalon and failing to navigate past to the optic tectum.

Our previous pharmacological study [18] did not speak of potential functional diversity of the different Fgfr isoforms, nor did it address whether Fgfs could directly impact guidance cue transcription in a cell-autonomous manner. To understand the receptor specificity by which Fgfs regulate guidance gene expression, we investigated in *Xenopus* the Fgf-dependent transcriptional control of the *slit1* gene in vitro and in vivo. We identified an Fgf-responsive 5'-regulatory region of *slit1* that could recapitulate spatiotemporal expression of endogenous *slit1* in the live embryo. Through expression analysis and molecular loss of function studies, we report that the *slit1* promoter has differential responses to signaling via distinct Fgfrs in vitro and in the forebrain. In the embryonic forebrain, *slit1* only depends on Fgfr1 activation. A similar dependence of *slit1* transcription on Fgfr1 signaling is true in kidney epithelial cells, despite the presence of Fgfr2/3, indicating that Fgfr1 controls *slit1* expression in vivo by activating a distinct signaling pathway from other Fgfrs.

Experimental procedures

X. laevis embryos

Eggs were collected from adult female *X. laevis* injected with human chorionic gonadotropin (Intervet) using established procedures [18]. The embryos were incubated at either 16 or 20 °C to control the rate of development [24]. All animal protocols were approved by the University of Calgary Animal Care Committee.

Identification of the *slit1* promoter and plasmid constructs

PCR primers were designed to isolate the -2285 to $+326$ *slit1* region (2.3 kb *slit1* promoter, GenBank accession number KP322597.1) using hepatic genomic DNA from *X. tropicalis* as template. The isolated *slit1* promoter was then cloned into the promoterless pGL3 (Promega) firefly luciferase reporter vector to yield $-2285 + 326slit1::luc$ and into the *pcDNA3.1-GFP* reporter vector to yield $-2285 + 326slit1::GFP$. Deletion fragments were amplified by PCR from $-2285 + 326slit1::luc$, using the primers in Supplementary Table S1. Deletion fragments were subcloned into pGL3. Plasmids were sequenced at the University of Calgary Core DNA facility.

The *Xenopus* constructs for dominant negative (DN) Fgfr1/2/4 and soluble Fgfr3 (sFgfr3) were *pCS2-DNfgfr1* [25], *pCS108-DNfgfr2*, pCS108-*sfgfr3*, and pCS2MTC-DN*fgfr4* [18, 26, 27]. The construct for *Xenopus* Fgf8 was *pCS2-xfgf8* [18].

X. laevis blastomere injection

Embryos at the two-cell stage were transferred to 4% Ficoll (GE Healthcare) in 1× modified Barth's saline (MBS; 0.7 mM CaCl$_2$, 5 mM HEPES, 1 mM KCl, 1 mM MgSO$_4$, 2.5 mM NaHCO$_3$, 88 mM NaCl, pH 7.8). For luciferase assays, the DNA solution (80 ng/μL, 3:1:1 ratio by weight consisting of the luciferase construct, normalizing *Renilla* luciferase construct, and *pCS2-GFP* for screening injected embryos) was injected into both blastomeres of the embryo. For in vivo assessment of the expression of the *slit1* reporter, $-2285 + 326slit1::GFP$ was injected alongside *pCS108-tdTomato* in a 2:1 w/w ratio, with tdTomato used to identify successful injections. A Picospritzer II (General Valve), equipped with a borosilicate needle, was used for injection. After injection, the embryos were transferred to 4% Ficoll

in 0.1× MBS overnight at 16 °C and then into 0.1× Mark's modified Ringer solution for development to the select stages.

Brain electroporation

Brain electroporation was performed according to established techniques [18, 28, 29]. A Picospritzer II (General Valve), equipped with a borosilicate needle, was used for injecting 1 μg/μL plasmid solution into the central forebrain ventricle of anesthetized Stage 27/28 embryos. The embryos were allowed to develop to Stage 32 to be analyzed quantitatively by qPCR or qualitatively by in situ hybridization.

Cell culture and transfection

A6 cells, *X. laevis* kidney epithelial cells [30] (provided by Dr. Lohka, University of Calgary) were cultured in 65% Leibovitz's L-15 (Life Technologies) media supplemented with 10% fetal bovine serum (Life Technologies). Cells were kept at 28 °C.

A6 cells were transfected at 80% confluency in black 96-well plates (Greiner Bio-One) with Lipofectamine 2000 (Life Technologies) according to the manufacturer's instructions. Briefly, 10 μL of Lipofectamine 2000 solution (10% solution diluted in serum-free L-15 media) was combined with 10 μL of DNA solution (100 ng of firefly luciferase reporter plasmid and 75 ng of *Renilla*). In the case of three-plasmid transfection, 50 ng of the third plasmid was included. Serum-free media was replaced with growing media 6 h after transfection and cells were harvested for luciferase assay at 48 h. For certain wells, 100 μM SU5402 (Sigma) was added 6 h after transfection.

Luciferase assay

The luciferase assay was conducted using the Dual-Glo Luciferase Assay System (Promega) according to the manufacturer's instructions. Luciferase and *Renilla* activity was measured by adding 30 μL of the luciferase substrate and Stop & Glo reagent, respectively. Luminescence was measured using a FilterMax F5 Multi-Mode Microplate Reader (Molecular Devices). The luciferase activity was normalized against *Renilla* and expressed as relative lights units over the promoterless pGL3 basic.

RNA isolation and RT-PCR

A6 cells and Stage 32 *X. laevis* embryonic forebrains were lysed in TRIzol (Life Technologies). Total RNA was extracted using the GeneJET RNA Purification Kit (Thermo Fisher).

cDNA was reverse transcribed from template RNA and primed with oligodT (Thermo Fisher), using SuperScript II Reverse Transcriptase (Thermo Fisher) according to the manufacturer's instructions.

For semi-quantitative RT-PCR, the genes of interest were amplified with PCR Master Mix (Thermo Scientific) with the primers in Supplementary Table S2.

qPCR was used to determine the relative gene expression using the CFX Connect Real-Time PCR Detection System (Bio-rad) and the CFX Manager Software v3.1 (Bio-rad). Primers are listed (Supplementary Table S3), along with their efficiencies and amplicon melt temperatures (Supplementary Table S4). qPCR was performed using the Quanti-Tect SYBR Green PCR Kit (Qiagen). Each 20 μL reaction contained 3 μL of reverse-transcribed cDNA solution, 2.5 μL of each forward and reverse primer (417 nM final concentration), 10 μL of SYBR Green QuantiTect RT-PCR master mix (Qiagen), and 2 μL water. The thermocycling parameters were: initial denaturing (95 °C, 10 min), denaturing (95 °C, 15 s), annealing (54 °C, 35 s), and elongation (72 °C, 30 s) for a total of 40 cycles. The melt curve was produced by heating the product to 95 °C in 0.5 °C increments. Gene expression was normalized to the reference genes beta-actin (*actb*), tubulin beta class I (*tubb*), and light chain dynein (*dynll1*) [31] using Relative Expression Software Tool 2009 V2.0.13 (Qiagen), which determined the statistical significance at $p < 0.05$.

Immunohistochemistry

Immunostaining was conducted according to [32]. Embryos were anesthetized in 0.01% tricaine, fixed overnight at 4 °C in 4% paraformaldehyde, immersed in 30% sucrose in PBS, mounted in OCT compound (Tissue Tek, Sakura Finetek, Inc., Torrance, CA, USA), and cryostat sectioned (12 μm thickness) prior to immunostaining. The primary antibody was rabbit anti-GFP IgG (1/1000 dilution, Molecular Probes Life Technologies A6455). The secondary antibody was goat anti-rabbit IgG conjugated to Alexa Fluor 488 (1/500 dilution, Molecular Probes Invitrogen R37116).

In situ hybridization (ISH)

Riboprobe synthesis and chromogenic ISH were conducted according to [32]. Anti-digoxigenin-AP Fab fragments (Roche 11 093 274 910) were used with BM Purple (Roche) for chromogenic visualization. For double fluorescent ISH, digoxigenin- and fluorescein- (Roche) labeled riboprobes were transcribed from linearized plasmid templates *pBSK-xfgfr1*, *pBSK-xBek-ec*, *pBSK-xfgfr3*, *pBSK-xfgfr4*, *pJet-xspry1*, and *pCMV-SPORT6-slit1* [26, 27, 33] using SP6 or T7 polymerase (Roche). The specificity of the riboprobes was analyzed previously through sense controls by others

for *fgfrs* [34], and by us for *spry1* and *slit1* (data not shown). Tissues were washed with anti-digoxigenin-POD (Roche 11 207 733 910) and anti-fluorescein-POD (Roche 11 426 346 910) and processed by the TSA Plus Fluorescein Evaluation Kit (PerkinElmer) and the TSA Cyanine 3 System (PerkinElmer) according to the manufacturer's instructions. ISH staining was visualized by the AxioCam HRc software (Carl Zeiss) on the Stemi SVII stereomicroscope (Carl Zeiss) at ambient temperature. Digital images were processed for brightness and contrast by using Adobe Photoshop (2017.0.0 release). Quantification of mRNA co-expression after in situ hybridization was performed only in the "regions of interest" highlighted in yellow in the cartoons (Fig. 1).

Statistical analysis

For luciferase data, we classified datasets as parametric or non-parametric based on whether the datasets satisfied the assumptions of ANOVA. First, we assumed the independence of errors, meaning that each technical and biological replicate were mutually independent. Then, the Anderson–Darling algorithm was used to assess the normality of the data. The *F* test and Bartlett's test were used to assess equal variances among treatment groups. We analyzed parametric data by Student's *t* test and analysis of variance (ANOVA) and non-parametric data by Mann–Whitney and Kruskal–Wallis tests on GraphPad Prism 7. The parametric post hoc test was Dunnett's test. Dunn's test was the non-parametric post hoc test.

Results

Spatiotemporal expression of *fgfr1–4* and *slit1*

We demonstrated previously in whole mount preparations that *fgfr1–4* and *slit1* are all expressed in the embryonic forebrain [18]. Not considered, however, was whether there was significant overlap at the cellular level between the expression of specific *fgfr* isoforms and *slit1*-positive forebrain domain. Here we address this issue, and whether the expression of *fgfrs* in the retina might also suggest a role for this signaling pathway in regulating retinal *slit1* expression [35]. We compared the expression patterns by double fluorescent in situ hybridization (ISH) of *fgfr1–4* and *slit1* in transverse sections through the brain and eye at Stage 32, a time when we showed Fgfr signaling positively regulated *slit1* forebrain expression [18]. At this stage, the first retinal ganglion cell (RGC) axons of the optic tract reach the optic chiasm and are en route to encounter Slit1 in the mid-diencephalon. In the retina, RGC and photoreceptor somata are starting to settle in their respective layers [36]. Proliferative cells are found dispersed throughout the neural retina, and progenitor
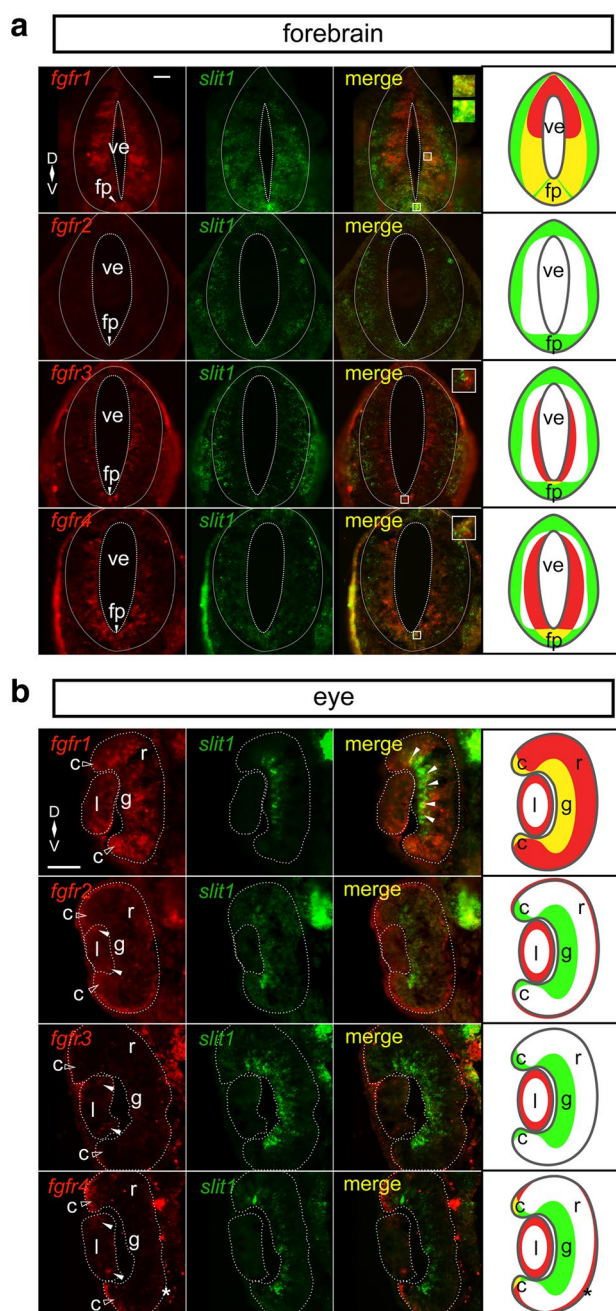

Fig. 1 *fgfr1–4* and *slit1* expression patterns in Stage 32 embryos. Double fluorescent in situ hybridization on transverse sections through the forebrain (**a**) and the eye (**b**) using specific antisense riboprobes against *fgfr1–4* and *slit1*. **a** There is co-expression of *slit1* and *fgfr1* ventrally adjacent to the ventricle and in the floor plate, *fgfr3* (floor plate), and *fgfr4* (floor plate). The insets focus on the regions of co-expression. **b** In the neural retina, *slit1* co-expresses with *fgfr1* in the presumptive retinal ganglion cell layer (white arrowheads) and ciliary marginal zone (unfilled arrowheads). The ciliary marginal zone (unfilled arrow heads) and the lens express different combinations of *fgfrs*, but not in conjunction with *slit1*. *fgfr2–4* expression in the lens is denoted by white arrowheads. The asterisk indicates *fgfr4* expression in the retinal pigmented epithelium. The dotted lines outline the boundaries of the ventricle, forebrain, lens, and neural retina. The rightmost column in each composite is a cartoon of the *fgfr* (red) and *slit1* (green) domains with co-expression in yellow. Scale bars 50 μm. *c* ciliary marginal zone, *fp* floor plate, *g* retinal ganglion cell layer, *l* lens, *r* neural retina, *ve* ventricle

populations are evident in the retinal periphery, as the ciliary marginal zone (CMZ), and at the periphery of the lens.

Only certain *fgfrs* were expressed by the cells that express *slit1*. We analyzed sections through the entire forebrain (Fig. 1a) and central retinal sections (Fig. 1b). Note that because of the distinct spatial expression patterns of the different *fgfr* isoforms in the forebrain, representative forebrain sections reflect those sections with maximal expression of the two genes being compared (i.e., may differ in the rostro-caudal axis), but assessments of co-expression were made from sections through the entire forebrain. In the forebrain, *slit1*-positive cells did not express *fgfr2*. Only the *fgfr1* ISH label showed significant amounts of overlap with the *slit1* signal. *fgfr1* and *slit1* were co-expressed ventrally by cells of the floor plate, and by neuroepithelial cells lining the ventricle, in particular at mid to ventral levels (co-expression shown in insets). In the region of interest, highlighted in yellow in the cartoon, virtually all (97.3%; 326/335, $N=3$) *slit1*-expressing cells also express *fgfr1*. In contrast, *slit1*-positive cells that were presumably post-mitotic and located at the basal side of the forebrain epithelium no longer expressed *fgfr1* mRNA, though Fgfr1 protein could still be present. *fgfr4* and *slit1* were mostly in separate populations of forebrain cells, though a small population of ventricular floor plate cells expressed both genes (co-expression shown in inset). *fgfr3* expression was restricted to more posterior forebrain sections. Here, it was mainly present in cells sitting next to the ventricles, whereas *slit1* was present in cells at the basal surface of the epithelium. Similar to *fgfr4*, *fgfr3* mRNA was present in a few floor plate cells alongside *slit1* (Fig. 1a; co-expression shown in inset). In these floor plate cells, all *slit1*-expressing cells express *fgfr3* (58/58, $N=3$) and *fgfr4* (42/42, $N=3$), respectively.

In the retina, *slit1* was expressed by cells in the proliferative CMZ (higher expression in ventral than dorsal CMZ), post-mitotic RGCs, and in what were likely to be cells specified to become RGCs that were migrating to the RGC layer (Fig. 1b). *fgfr1* mRNA was present in all of these populations. In the CMZ, all *slit1*-expressing cells also express *fgfr1* (68/68, $N=3$). In RGCs and cells migrating to the RGC layer, the vast majority of cells co-express *slit1* and *fgfr1* (96.5%; 165/171, $N=3$). In contrast, with the exception of co-expression of *slit1* and *fgfr4* in the CMZ (95.1%; 39/41 *slit1*-expressing cells, $N=3$), *fgfr2–4*-expressing cells of the eye did not express *slit1*. *fgfr2–4* were expressed by the proliferative cells of the lens, *fgfr2* and *fgfr4* by the retinal pigmented epithelium outlining the neural retina, and *fgfr4* by the CMZ (Fig. 1b). The presence of *fgfr4* in the lens, retinal pigmented epithelium, and CMZ is consistent with that of zebrafish at 36 h post-fertilization [37, 38].

These data indicate that multiple Fgfrs are positioned to control *slit1* expression by the floor plate. Only *fgfr1*, however, is significantly co-expressed by forebrain and retinal cells that express *slit1*. These data argue that Fgfr1 is the prime candidate to control Slit1 in a cell-autonomous manner in the forebrain. Nonetheless, in forebrain sections, *fgfr3* and *fgfr4*-expressing cells are present alongside *slit1*-positive cells. Thus, we cannot exclude the possibility that the protein for the receptors persists in the basally located post-mitotic *slit1*-positive cells.

slit1 promoter sequence has neural tube- and eye-specific expression elements

To study the transcriptional regulation of *slit1*, we identified approximately 2.3 kb upstream of the *slit1* transcription start site, from *Xenopus tropicalis* genomic DNA. We tested promoter activity in the 5′-flanking sequence by a luciferase reporter system. The luciferase reporter construct $-2285+326slit1::luc$ showed 20 times more activity than the promoterless pGL3 basic vector when injected into both cells of *X. laevis* blastomeres at the two-cell stage and analyzed at stage 12 (Fig. 2a, b).

To analyze whether tissue-specific regulatory elements were present in the identified *slit1* promoter sequence, we inserted the 2.3 kb *slit1* promoter upstream of *GFP* cDNA to generate the $-2285+326slit1::GFP$ reporter construct. This GFP reporter was injected into both blastomeres of the *X. laevis* two-cell embryo. The embryos were allowed to develop to Stage 32, at which time we compared the expression of the reporter GFP, assessed immunohistochemically, with endogenous expression of *slit1* mRNA. Of note, the ISH for endogenous mRNA captures expression within a short time period, while GFP represents summed expression over time due to the considerably longer half-life of GFP protein compared to *slit1* mRNA. Further, while mRNA is generally localized to the nucleus and cell body, GFP labels the entire cytoplasmic extent of cells. Finally, GFP expression driven by the *slit1* promoter in plasmid-injected embryos would be mosaic in nature, as is the case for cDNA plasmids injected into blastomeres of the two-cell embryo.

We co-injected into *X. laevis* blastomeres $-2285+326slit1::GFP$ along with *pCS108-tdTomato*, driven by the ubiquitous CMV promoter (Fig. 2a). tdTomato protein was expressed throughout the forebrain and the eye (Fig. 2c, g), exhibiting no tissue specificity. In contrast, the GFP-positive domains made up a subset of the tdTomato expressing cells, indicating that the *slit1* promoter has tissue specificity (Fig. 2d, h). The GFP-immunostained sections revealed expression that was similar to that of *slit1* mRNA (Fig. 2e, i). The identified *slit1* promoter was active in characteristic *slit1* mRNA expression domains, i.e., the floor plate in the forebrain and the cells that radially span the neural retina (presumptive RGCs).

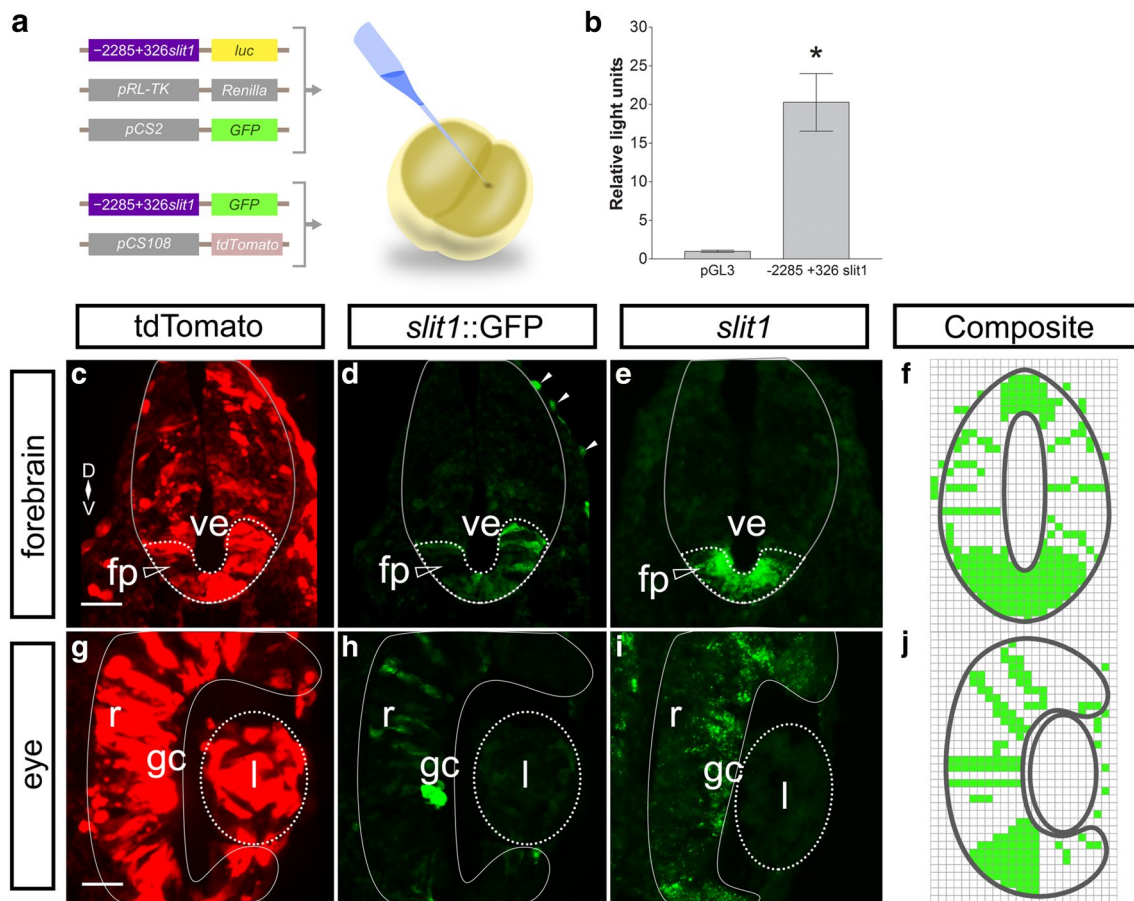Out of a total of 22 injected embryos, 17 expressed mosaic GFP in the neural tube and eye similar to the

Fig. 2 Identifying a functional *slit1* promoter in *X. laevis* embryos. **a** The *slit1* 5′-flanking region was inserted upstream of the firefly luciferase (*luc*) construct in the pGL3 basic vector, −2285 + 326 *slit1::luc*, and co-injected into *X. laevis* embryos with the *Renilla* luciferase vector. **b** The firefly luciferase luminescence was normalized against the *Renilla* luciferase luminescence and expressed with respect to the promoterless luciferase vector pGL3 basic. Bars reflect mean ± SEM from 29 embryos in five independent experiments. *$p < 0.05$, Mann–Whitney test compared to pGL3 basic. **a** The −2285 + 326 *slit1::GFP* reporter and *pCS108-tdTomato* were co-injected into *X. laevis* blastomeres. Transverse sections through the Stage 32 forebrain (**c**) and eye (**g**) show near ubiquitous expres-sion of tdTomato, but restricted expression of GFP (**d** and **h**, white arrowheads denote ectopic GFP expression). GFP expression was comparable to the *slit1* in situ hybridization (**e** and **i**) in the floor plate and the presumptive retinal ganglion cell layer of the neural retina. The solid outline marks the boundary of the neural tube (**c**–**e**) and the neural retina (**g**–**i**). The dotted outline encircles the floor plate (**c**–**e**, unfilled arrowhead) and the lens (**g**–**i**). The mosaic GFP expression from −2285 + 326 *slit1::GFP* embryos, $n = 17$ from three independent experiments, was combined into composites (**f** and **j**). Scale bars 50 μm. *fp* floor plate, *gc* retinal ganglion cell layer, *l* lens, *r* neural retina, *ve* ventricle

example in Fig. 2d, h. The mosaic expression patterns of the 17 embryos were combined into composites (Fig. 2f, j). These results suggest that important *cis*-regulatory elements controlling *slit1* expression in the neural tube and retina are present in the 2.3 kb *slit1* promoter. Since the *slit1* promoter was cloned from *X. tropicalis* DNA, these data also indicate that the regulatory regions of the *slit1* gene are conserved between *X. laevis* and *X. tropicalis*.

Characterization of the *slit1* promoter

Knowing that the identified *slit1* promoter drives tissue-specific expression similar to the endogenous mRNA, we then further characterized the promoter and tested its ability to respond to Fgf signaling in a cell-autonomous manner in vitro. To identify regulatory elements in the *slit1* promoter, we performed a bidirectional deletion analysis of the 2.3 kb *slit1* sequence (Fig. 3a) by using the A6 epithelial cell line from adult frog kidney [30]. First, we verified by RT-PCR that A6 cells endogenously express *slit1* (Fig. 3b), which would argue that the cells have the proper regulatory mechanisms for studying *slit1* transcriptional control.

The *slit1* deletion fragments driving reporter luciferase were co-transfected with the *Renilla* luciferase construct. The *Renilla* luciferase construct, driven by the ubiquitous tyrosine kinase promoter, served to normalize transfection
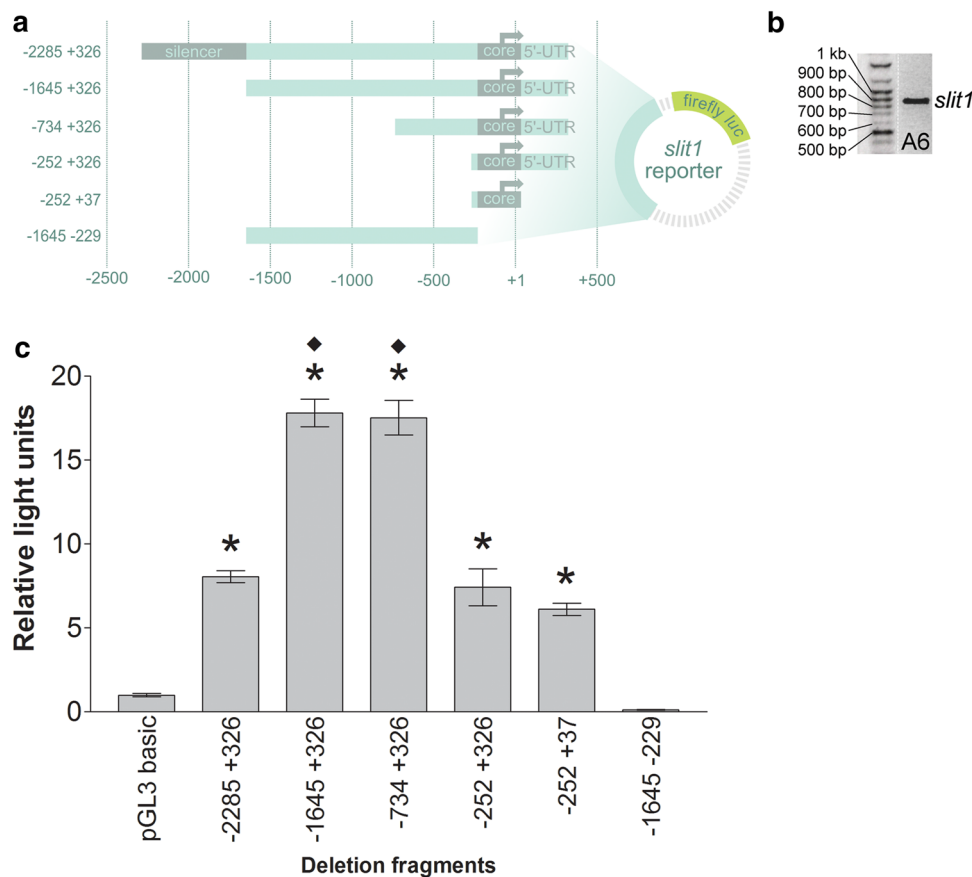
Fig. 3 Deletion analysis of the identified *slit1* promoter in A6 cells. **a** Schematic representation of the deletion fragments from the *slit1* 5′-flanking region cloned upstream of the reporter firefly luciferase (*luc*) cDNA in the pGL3 basic vector. **b** Endogenous expression of *slit1* in A6 cells was confirmed by RT-PCR. **c** A6 cells were co-transfected transiently with the *slit1::luc* deletion constructs and the *Renilla* luciferase plasmid to normalize transfection efficiency. Cells were harvested 48 h after transfection. Promoter activity was calculated as luciferase activity over *Renilla* activity and expressed as the ratio over that of pGL3 basic promoterless vector (relative lights units). Bars reflect mean $\pm$ SEM from $n = 236$ wells from 13 independent experiments. Statistical significance was determined by Kruskal–Wallis test followed by $*p < 0.01$ comparison with pGL3 basic (Dunn's post hoc test) and $\blacklozenge p < 0.001$ comparison with $-2285 + 326 slit1::luc$ (Dunn's post hoc test)

efficiency. Promoter activity was quantified by luciferase assay. A 3′-deletion of the *slit1* reporter showed that the minimal promoter region (core promoter) was located between nucleotides -229 and $+37$, since the -252 to $+37$ construct remained functional while the region -1645 to -229 did not (Fig. 3c). From the 5′-end, the *slit1* regulatory region has silencing activity between nucleotides -2285 and -1645, as deletion of this region increased promoter activity approximately twofold (compare constructs $-2285 + 326 slit1::luc$ vs. $-1645 + 326 slit1::luc$ and $-734 + 326 slit1::luc$). Therefore, the 2.3 kb *slit1* promoter contains a core promoter and a silencer.

Fgf signaling transcriptionally regulates *slit1*

We next focused on the possible regulation of *slit1* transcription by Fgf signaling. Our previous work showed that Fgf signaling maintains *slit1* expression in the *X. laevis* forebrain [18], but did not establish whether Fgf regulated *slit1* transcription in a cell-autonomous manner, and which Fgfrs were involved. We took advantage of the luciferase assay in A6 cells to address these issues. First, we established by RT-PCR that all *fgfrs* were detected in A6 cells, including two forms for receptors 1 and 4 (1a–b and 4a–b) (Fig. 4a). All PCR amplicons of approximately 900 bp corresponded to the indicated *fgfr*, as confirmed by sequencing, with the exception of *fgfr1b* amplicons smaller than 900 bp, which might have been alternatively spliced transcripts [39], but were not sequenced.

It was important to verify that the 2.3 kb regulatory sequence we had identified was responsive to Fgf signaling. To do so, we treated A6 cells with a well-characterized Fgfr inhibitor, SU5402 [40] (Fig. 4b). SU5402 at 100 µM significantly decreased the promoter activity of the *slit1*
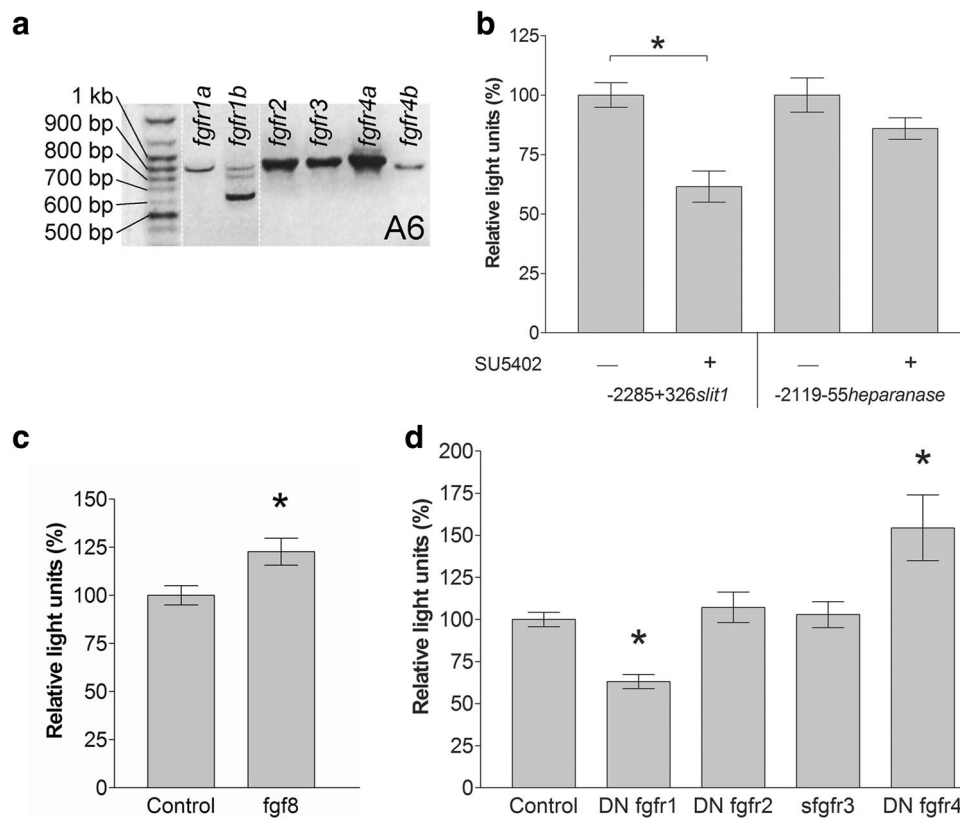
Fig. 4 The *slit1* promoter responds to Fgfr manipulation in A6 cells. **a** Expression of *fgfrs* in A6 cells was assessed by RT-PCR. **b** The $-2285+326$ *slit1::luc* and $-2119-55heparanase::luc$ reporters were each transfected into A6 cells and incubated with 100 μM of the Fgfr inhibitor, SU5402, for 42 h. Luminescence is expressed as a percentage of the control (DMSO) without SU5402. Bars represent the mean $\pm$ SEM for $n=123$ wells from six independent experiments. $^*p<0.05$ ANOVA followed by Dunnett's post hoc test compared with control. The $-2285+326$ *slit1::luc* reporter was co-transfected with *pCS2-xfgf8* (**c**) or constructs for truncated Fgfrs (**d**). Luminescence is expressed as a percentage of the control (*pCS2-GFP*). Bars represent the mean $\pm$ SEM for $n=16$ wells from four independent experiments (**c**) and $n=98$ wells from nine independent experiments (**d**). $^*p<0.05$ two-tailed Student's t test compared with control (**c**) and $p<0.05$ Kruskal–Wallis test followed by Dunn's post hoc test compared with control (**d**)

reporter construct, but did not affect the heparanase promoter construct, $-2119-55heparanase::luc$, used as the negative control [41]. Further, co-transfection of *pCS2-xfgf8* with $-2285+326slit1::luc$ significantly increased promoter induction (Fig. 4c). Thus, the *slit1* regulatory sequence contained the necessary elements to respond to Fgf signals.

To identify the specific Fgfrs that regulate *slit1* expression, we took a molecular approach to inhibit Fgfrs. We used truncated Fgfrs: dominant negative Fgfr1/2/4 (DN Fgfr1/2/4) and soluble Fgfr3 (sFgfr3), all from *Xenopus*, which inhibit Fgf signaling through their wild-type counterparts [18, 25–27]. The dominant negative receptors contain the extracellular and intramembrane domains, but lack the catalytic intracellular domain. The soluble Fgfr3 has only the extracellular domain.

The effects of each truncated Fgfr at blocking *slit1* induction were analyzed by co-transfection of A6 cells with each one of the DN *fgfr1/2/4* and *sfgfr3* expression constructs together with the 2.3 kb *slit1* luciferase reporter construct

(Fig. 4d). The promoter activity of *slit1* was not affected by co-transfection with the DN *fgfr2* or *sfgfr3*. Interestingly, blockade of Fgfr1 and Fgfr4 reduced and stimulated *slit1* promoter induction, respectively. These data suggest that Fgf signaling regulates *slit1* transcription through select Fgfr pathways. Moreover, *slit1* expression appears to be regulated differentially by the particular receptor that is activated.

Transcriptional regulation of forebrain *slit1* is mediated by Fgfr1 signaling

To identify in vivo the Fgfrs that control *slit1* expression in the embryonic forebrain, the same truncated Fgfrs used in vitro were electroporated into the right half of the forebrain of *X. laevis* embryos at Stage 27/28. The *pCS2-GFP* plasmid served as electroporation control. The majority of cells in the electroporated side of the forebrain expressed each of the truncated *fgfrs*, as assessed by ISH (Fig. 5a, b). We first assessed in a qualitative manner *slit1* expression in

DN *fgfr*-electroporated embryos by ISH. Only expression of the DN Fgfr1 affected *slit1* expression, with *slit1* signal being noticeably decreased in multiple domains of the diencephalon and telencephalon as compared to the control (Fig. 5c, d). The other DN Fgfr constructs did not impact *slit1* expression. These data agree with the in vitro A6 cell data where DN Fgfr1 decreased *slit1* promoter activity.

To verify the ISH data, we quantified changes in *slit1* expression by qPCR. Importantly, *spry1*, the negative feedback regulator of Fgf signaling, was reduced with each one of the *fgfr* inhibition constructs [18, 42] (Supplementary Fig. S1; Fig. 5e), arguing that the constructs effectively blocked Fgf signaling. In agreement with the ISH data, qPCR revealed that *slit1* expression was significantly reduced by blocking signaling by Fgfr1, but not Fgfr2–4. Therefore, in both A6 epithelial cells and the developing forebrain, it seems that Fgfr1 is a key regulator of *slit1*.

Discussion

Axon guidance cues are expressed at strategic times and locations to direct growing axons toward their post-synaptic targets. For instance, Slit1/2 guides optic tract development [43, 44], controls the development of RGC dendrites [45], and facilitates commissural and longitudinal axon pathfinding in the forebrain [46–48]. Currently, not much is known about the transcriptional regulation of guidance cues during embryogenesis. In *Xenopus*, Fgf signaling is required to maintain *slit1* expression throughout the anterior brain [18]. Here, we build on our previous work to identify for the first time in vivo a specific growth factor receptor which controls the expression of a guidance cue, providing novel insight into how extrinsic signals function in the developing brain to control the map of molecular cues that guide growing axons. Specifically, we identify: (1) that Fgf signaling regulates *slit1* expression transcriptionally and most likely in a cell-autonomous manner; (2) the *slit1* promoter recapitulates endogenous expression in the forebrain and the eye and contains the necessary elements to respond to Fgf signals, and (3) via expression analysis and in vitro and in vivo molecular loss of function studies that the Fgf signal is specifically mediated by Fgfr1.

The observation that the *slit1* promoter sequence obtained from *X. tropicalis* recapitulates the endogenous spatiotemporal mRNA expression in *X. laevis* argues for conservation in transcriptional regulatory activity between *Xenopus* species. Interestingly, the expression pattern we observe in *X. laevis* for *slit1* is similar to that observed in rat and chick, especially the characteristic *slit1* domain in the floor plate [49, 50]. These data suggest *slit1* expression is conserved among multiple species even though the *Xenopus slit1* promoter sequence does not show high homology by alignment
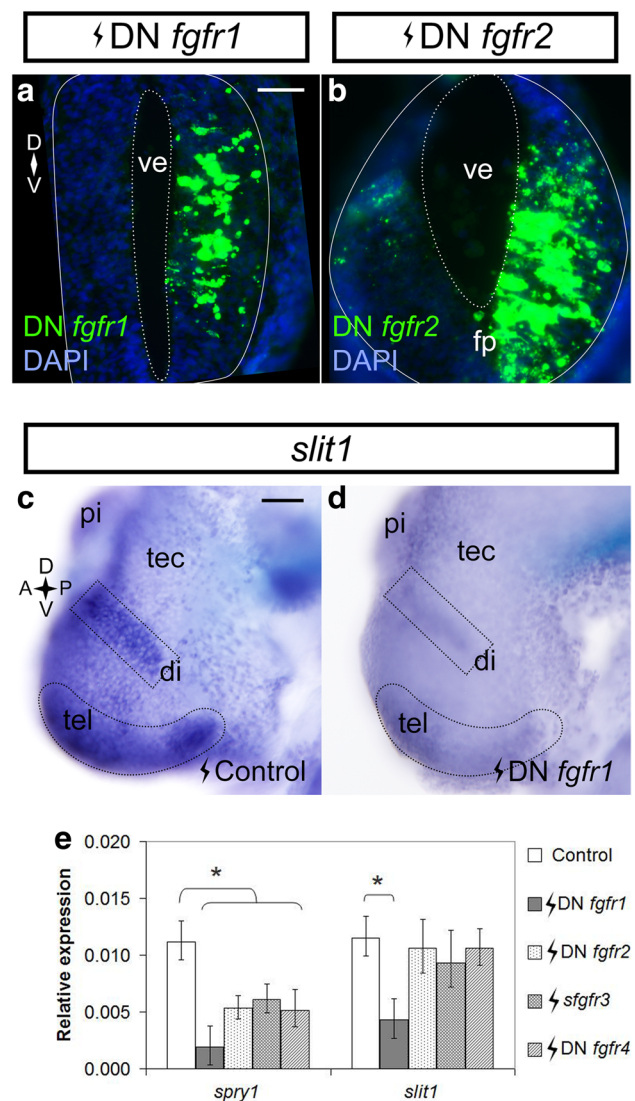

Fig. 5 Fgfr1 inhibition downregulates *slit1* in the forebrain. Stage 27/28 embryos were electroporated in the forebrain with *pCS2*-DN*fgfr1* (**a**) and *pCS108*-DN*fgfr2* (**b**) and processed in transverse sections for *fgfr1/2* in situ hybridization at Stage 32 to reveal the expression of the constructs. In **a** and **b**, the solid outline encircles the neural tube, and the dotted outline borders the ventricle. Stage 27/28 embryos were electroporated with control *pCS2-GFP* (**c**) (*n* = 13 embryos from two independent experiments) or *pCS2*-DN*fgfr1* (**d**) (*n* = 12 embryos from two independent experiments; 10/12 brains showed downregulation) and processed for *slit1* expression by whole mount in situ hybridization at Stage 32. The dotted outlines in **c** and **d** indicate the *slit1* domains of interest. **e** The *slit1* expression in the brains of embryos electroporated with truncated *fgfrs* was measured by qPCR. *spry1* was a readout of Fgfr inhibition. Bars represent mean ± SEM for *n* = 137 embryos from four independent experiments. *$p < 0.05$ statistical significance versus the control was determined using the REST 2009 algorithm. Scale bars 50 μm. *di* diencephalon, *fp* floor plate, *pi* pineal gland, *tec* optic tectum, *tel* telencephalon, *ve* ventricle

of the sequences from human, rat, or chick (NCBI BLAST and ConBind Motif-Aware Phylogenetic Footprinting, data not shown).

Of note, while the *X. tropicalis slit1* promoter recapitulates endogenous *X. laevis* mRNA expression patterns, the sequence also drives ectopic reporter GFP expression in some skin cells. Thus, the 2.3 kb *slit1* promoter sequence likely does not fully capture the domains that repress expression in the skin, but is sufficient for expression in the neural tube and retina. Importantly, for our studies, the sequence also contains the domains necessary for responsiveness to Fgf signals.

We found previously that Fgfr signaling maintains the expression of *slit1* in the *Xenopus* forebrain [18], in that, transient in vivo pharmacological inhibition of Fgfrs by SU5402 rapidly downregulates *slit1* transcripts in the embryonic forebrain within hours. Unclear, however, was whether Fgf-dependent regulation of *slit1* expression occurred in a cell-autonomous manner, or whether Fgfs stimulated the production and secretion of an extrinsic factor that then controlled *slit1* mRNA levels in neighboring cells. The rapid speed of the downregulation of *slit1* (6 h or less) with pharmacological Fgfr inhibition [18] argues for a more direct regulation of expression by Fgfr signaling, as does the fact that forebrain cells and A6 cells co-express *fgfrs* and *slit1*. Moreover, molecular inhibition of Fgfr signaling in A6 cells downregulates *slit1* promoter activity, despite the fact that the efficiency of transfection is sufficiently low (around 30% for all constructs, data not shown) that the large non-transfected population of A6 cells would continue to provide any key secreted signal. Thus, the data support cell-autonomous regulation of *slit1* gene expression by an Fgf signaling pathway.

Intriguingly, we find both in vitro and in vivo that signaling downstream of only certain Fgfrs regulates *slit1* expression. Only *fgfr1*, and, to a much lesser extent *fgfr3/4* in the floor plate, is co-expressed along with *slit1* by forebrain neuroepithelial cells, indicating that Fgfr1 could be particularly key in controlling *slit1* transcription. In agreement, manipulating Fgfr1 function revealed that Fgfr1 in both A6 cells and the *Xenopus* forebrain positively regulated *slit1* expression, while inhibition of Fgfr2/3 had no impact on *slit1* levels, even though the mRNA levels of the *spry1* Fgfr signaling feedback mediator [42] were downregulated by the expression of Fgfr2/3 truncated receptors. The mRNA expression data indicate that possibly the failure of Fgfr2/3 to control *slit1* levels in *slit1*-expressing forebrain neuroepithelial cells is because the receptors are largely absent from the cells. The A6 cell data, however, argue that signaling through Fgfr2/3 is simply unable to regulate expression. A6 cells express all of the *fgfrs*, but only Fgfr1/4 inhibition impacts *slit1* promoter activity. Thus, the signaling pathway that functions downstream of Fgfr1 is potentially sufficiently

distinct from those that are active downstream of Fgfr2/3 [51], such that only the former can control *slit1* gene activity.

The upregulation of the *slit1* promoter in A6 cells transfected with DN Fgfr4 suggests that Fgfr4 may also control *slit1* expression. However, the data show that Fgfr4 signaling normally inhibits rather than promotes *slit1* promoter activity. A possible explanation for this discrepancy is the strength of the response generated by Fgfr1 and Fgfr4 [52], in that although Fgfr1 and Fgfr4 compete for Fgf ligands, downstream Fgf signaling is evoked more strongly by Fgfr1 than Fgfr4 activation. Such is the case for the effect of Fgfr1/4 signaling on *pax2* expression at the *Xenopus* midbrain–hindbrain boundary [52, 53]. Thus, in A6 cells, the DN Fgfr4 and DN Fgfr1 might both exert their effects through modulation of Fgfr1 signaling pathway: the DN Fgfr1 would effectively inhibit signaling through the wild-type Fgfr1, while the DN Fgfr4, by eliminating the Fgfr4 signaling pathway, would allow the stronger Fgfr1 signaling pathway to prevail, and would be seen as activation of Fgfr signaling. The result would be induction of *slit1* promoter activity.

Whether Fgfr4 also normally inhibits forebrain *slit1* transcription is debatable. First, while *fgfr1* is co-expressed by a significant number of *slit1*-expressing forebrain cells, *fgfr4* and *slit1* are co-expressed by only a subset of floor plate cells. Nevertheless, we cannot exclude the possibility that a control of *slit1* forebrain mRNA levels by Fgfr4 was not revealed in our experiments either because we failed to target the small domain of *fgfr4/slit1* co-expression with the truncated receptor, or that changes in *slit1* mRNA levels in this small domain contributed only a small degree to the amount of *slit1* in the anterior brain as measured by qPCR. In combination, however, the functional and expression data argue that Fgfr4 is not a significant regulator of *slit1* transcription.

The fact that we observed regulation of *slit1* transcription by Fgfr1 and not Fgfr2/3 in both mature kidney epithelial cells and embryonic forebrain argues for the generalizability of Fgfr1-dependent *slit1* expression. Testing whether Fgfr1 controls *slit1* expression by RGCs would help explore this idea further. Also, since *Fgfr1* is expressed by progenitors lining the ventricle of the mouse forebrain [54], similar to our *fgfr1* mRNA domain in the *Xenopus* forebrain, *Slit1* may similarly be controlled by FGF signaling in mammals. In rats, however, forebrain progenitor cells also express *Fgfr2*, but not *Fgfr3/4* [55]. Thus, unlike in *Xenopus* where Fgfr2 appears to play no role in controlling *slit1* transcription, in mammals Fgfr2 is a potential participant. Nonetheless, Fgfr2 may not do so, if, as we find in *Xenopus* A6 cells, the downstream signaling pathways do not link Fgfr2 to control of the *slit1* gene.

Interestingly, *slit1* and *fgfr1* mRNA are co-expressed likely by the neural progenitor cells of the ventricular

zone of the forebrain, while *slit1* is expressed toward the basal face where post-mitotic cells reside. Thus, it appears that *slit1* is positively regulated in progenitors in an *fgfr1*-dependent fashion, and *slit1* continues to be expressed as neurons are born and move away from the ventricular zone, even as *fgfr1* expression turns off. Presumably, the Fgfr1 protein continues to be expressed in the post-mitotic cells for a period, and we propose that it maintains high *slit1* levels. Eventually, however, *slit1* must become independent of Fgf signaling, given that we find *slit1* continues to be expressed by the *Xenopus* forebrain into the larval period (data not shown).

The involvement of guidance cues and their receptors in cancer has been well studied [2, 56]. Here, the dysregulation of guidance molecule expression is correlated with tumorigenesis and prognosis. For instance, dysregulation of Slit2 levels stimulates angiogenesis and cell motility [57–59], and increased Slit-Robo signaling can promote cancer [60–62]. Slit and Robo, however, also have tumor-suppressive roles [54, 61, 62]. In various cancers, *SLIT1–3* are epigenetically silenced by hypermethylation of the promoter [5, 6, 63, 64], and in neuroblastomas, NeuroD1 directly binds to the *SLIT2* promoter to repress transcription [65]. Yet, for both *SLIT* and other axon guidance cue genes, the signaling pathways and the transcription factors that control gene transcription in cancer, just as in development, are largely unknown. Interestingly, Slit can control its own expression. For instance, as cells extrude aberrantly from the main epithelial disc of *Drosophila*, c-Jun N-terminal kinase, Slit, and Robo2 form a positive feedback loop to increase Slit expression [66]. It is noteworthy that Slits, Semaphorins, and Ephrins, among other guidance molecules, are upregulated at the site of injury in the central nervous system, though the signals involved are largely unknown [67, 68].

Our data identify an extrinsic signaling pathway involving Fgfr1 that appears to work in a cell-autonomous fashion to control *slit1* expression in the developing forebrain. In future, we can use our experimentally accessible in vivo *Xenopus* forebrain model to ask whether other axon guidance cues are similarly controlled by Fgfs, and specifically Fgfr1, and the identity of the signal transduction pathways and transcription factors that act downstream of Fgfr1 to control *slit1* expression. In summary, our work provides a basis to explore how guidance cues may be regulated in development, cancer, and injury.

Compliance with ethical standards

References

1. McFarlane S, Lom B (2012) The *Xenopus* retinal ganglion cell as a model neuron to study the establishment of neuronal connectivity. Dev Neurobiol 72(4):520–536

2. Chédotal A, Kerjan G, Moreau-Fauvarque C (2005) The brain within the tumor: new roles for axon guidance molecules in cancers. Cell Death Differ 12:1044–1056

3. Dickson B (2002) Molecular mechanisms of axon guidance. Science 298:1959–1964

4. James G, Foster SR, Key B, Beverdam A (2013) The expression pattern of EVA1C, a novel slit receptor, is consistent with an axon guidance role in the mouse nervous system. PLoS One 8(9):e74115.1–e74115.10

5. Yu J, Cao Q, Yu J, Wu L, Dallol A, Li J, Chen G, Grasso C, Cao X, Lonigro R, Varambally S, Mehra R, Palanisamy N, Wu J, Latif F, Chinnaiyan A (2010) The neuronal repellent SLIT2 is a target for repression by EZH2 in prostate cancer. Oncogene 29(39):5370–5380

6. Dickinson RE, Dallol A, Bieche I, Krex D, Morton D, Maher E, Latif F (2004) Epigenetic inactivation of SLIT3 and SLIT1 genes in human cancers. Br J Cancer 91:2071–2078

7. Narayan G, Goparaju C, Arias-Pulido H, Kaufmann AM, Schneider A, Dürst M, Mansukhani M, Pothuri B, Murty VV (2006) Promoter hypermethylation-mediated inactivation of multiple Slit-Robo pathway genes in cervical cancer progression. Mol Cancer 5:16

8. Aldiri I, Moore KB, Hutcheson KA, Zhang J, Vetter ML (2013) Polycomb repressive complex PRC2 regulates *Xenopus* retina development downstream of Wnt/β-catenin signaling. Development 140:2867–2878

9. Aldiri I, Vetter ML (2012) PRC2 during vertebrate organogenesis: a complex in transition. Dev Biol 367(2):91–99

10. Zarin AA, Asadzadeh J, Labrador JP (2014) Transcriptional regulation of guidance at the midline and in motor circuits. Cell Mol Life Sci 71:419–432

11. Inamata Y, Shirasaki R (2014) Dbx1 triggers crucial molecular programs required for midline crossing by midbrain commissural axons. Development 141:1260–1271

12. Miyashita T, Yeo S, Hirate Y, Segawa H, Wada H, Little M, Yamada T, Takahashi N, Okamoto H (2004) PlexinA4 is necessary as a downstream target of Islet2 to mediate Slit signaling for promotion of sensory axon branching. Development 131:3705–3715

13. Tang K, Rubenstein JL, Tsai SY, Tsai MJ (2012) COUP-TFII controls amygdala patterning by regulating neuropilin expression. Development 139:1630–1639

14. Lodato S, Molyneaux BJ, Zuccaro E, Goff LA, Chen HH, Yuan W, Meleski A, Takahashi E, Mahony S, Rinn JL, Gifford DK, Arlotta P (2014) Gene co-regulation by Fezf2 selects neurotransmitter identity and connectivity of corticospinal neurons. Nat Neurosci 17:1046–1054

15. Strähle U, Fischer N, Blader P (1997) Expression and regulation of a netrin homologue in the zebrafish embryo. Mech Dev 62:147–160

16. Hörndli CS, Chien CB (2012) Sonic hedgehog is indirectly required for intraretinal axon pathfinding by regulating chemokine expression in the optic stalk. Development 139:2604–2613

17. Barresi MJF, Hutson LD, Chien CB, Karlstrom RO (2005) Hedgehog regulated Slit expression determines commissure and glial cell position in the zebrafish forebrain. Development 132:3643–3656

18. Atkinson-Leadbeater K, Bertolesi GE, Hehr CL, Webber CA, Cechmanek PB, McFarlane S (2010) Dynamic expression of axon guidance cues required for optic tract development is controlled by fibroblast growth factor signaling. J Neurosci 30:685–693

19. Tsai PS, Brooks LR, Rochester JR, Kavanaugh SI, Chung WCJ (2011) Fibroblast growth factor signaling in the developing neuroendocrine hypothalamus. Front Neuroendocrinol 32(1):95–107

20. Turner N, Grose R (2010) Fibroblast growth factor signaling: from development to cancer. Nat Rev Cancer 10:116–129

21. Eswarakumar VP, Lax I, Schlessinger J (2005) Cellular signaling by fibroblast growth factor receptors. Cytokine Growth Factor Rev 16:139–149

22. Yamauchi K, Mizushima S, Tamada A, Yamamoto N, Takashima S, Murakami F (2009) FGF8 signaling regulates growth of midbrain dopaminergic axons by inducing semaphorin 3F. J Neurosci 29(13):4044–4055

23. Shamim H, Mahmood R, Logan C, Doherty P, Lumsden A, Mason I (1999) Sequential roles for Fgf4, En1 and Fgf8 in specification and regionalisation of the midbrain. Development 126:945–959

24. Faber J, Nieuwkoop P (1994) Normal table of *Xenopus laevis* (Daudin): a systematical and chronological survey of the development from the fertilized egg till the end of metamorphosis. Garland Publishing, New York

25. Ueno H, Gunn M, Dell K, Tseng A, Williams L (1992) A truncated form of fibroblast growth factor receptor 1 inhibits signal transduction by multiple types of fibroblast growth factor receptor. J Biol Chem 267:1470–1476

26. Atkinson-Leadbeater K, Hehr C, McFarlane S (2014) Fgfr signaling is required as the early eye field forms to promote later patterning and morphogenesis of the eye. Dev Dyn 243:663–675

27. Golub R, Adelman Z, Clementi J, Weiss R, Bonasera J, Servetnick M (2000) Evolutionarily conserved and divergent expression of members of the FGF receptor family among vertebrate embryos, as revealed by FGFR expression patterns in *Xenopus*. Dev Genes Evol 210:345–357

28. Chen YY, Hehr CL, Atkinson-Leadbeater K, Hocking JC, McFarlane S (2007) Targeting of retinal axons requires the metalloproteinase ADAM10. J Neurosci 27:8448–8456

29. Haas K, Jensen K, Sin WC, Foa L, Cline HT (2002) Targeted electroporation in *Xenopus* tadpoles in vivo: from single cells to the entire brain. Differentiation 70:148–154

30. Rafferty KJ, Sherwin RW (1969) The length of secondary chromosomal constrictions in normal individuals and in a nucleolar mutant of *Xenopus laevis*. Cytogenetics 8:427–438

31. Brunsdon HR (2015) An analysis of FGF-regulated genes during *Xenopus* neural development. Dissertation, University of York

32. Sive H, Grainger RM, Harland RM (2000) Early development of *Xenopus laevis*: a laboratory manual. Cold Spring Harbor Laboratory Press, New York

33. Atkinson-Leadbeater K, Bertolesi GE, Johnston JA, Hehr CL, McFarlane S (2009) FGF receptor dependent regulation of Lhx9 expression in the developing nervous system. Dev Dyn 238:367–375

34. Hongo I, Kengaku M, Okamoto H (1999) FGF signaling and the anterior neural induction in *Xenopus*. Dev Biol 216:561–581

35. Hocking JC, Hehr CL, Bertolesi GE, Wu JY, McFarlane S (2010) Distinct roles for Robo2 in the regulation of axon and dendrite growth by retinal ganglion cells. Mech Dev 127(1–2):36–48

36. Holt CE, Bertsch TW, Ellis HM, Harris WA (1988) Cellular determination in the *Xenopus* retina is independent of linear and birth date. Neuron 1:15–26

37. Russell C (2002) The roles of hedgehogs and fibroblast growth factors in eye development and retinal cell rescue. Vis Res 43:899–912

38. Sleptsova-Friedrich I, Li Y, Emelyanov A, Ekker M, Korzh V, Ge R (2001) fgfr3 and regionalization of anterior neural tube in zebrafish. Mech Dev 102(1–2):213–217

39. Friesel R, Dawid I (1991) cDNA cloning and developmental expression of fibroblast growth factor receptors from *Xenopus laevis*. Mol Cell Biol 11:2481–2488

40. Mohammadi M, McMahon G, Sun L, Tang C, Hirth P, Yeh B, Hubbard S, Schlessinger J (1997) Structures of the tyrosine kinase domain of fibroblast growth factor receptor in complex with inhibitors. Science 276:955–960

41. Bertolesi GE, Su HY, Michaiel G, Dueck SM, Hehr CL, McFarlane S (2011) Two promoters with distinct activities in different tissues drive the expression of heparanase in *Xenopus*. Dev Dyn 240:2657–2672

42. Hacohen N, Kramer S, Sutherland S, Hiromi Y, Krasnow MA (1998) sprouty encodes a novel antagonist of FGF signaling that patterns apical branching of the *Drosophila* airways. Cell 92(2):253–263

43. Plump A, Erskine L, Sabatier C, Brose K, Epstein C, Goodman C, Mason C, Tessier-Lavigne M (2002) Slit1 and Slit2 cooperate to prevent premature midline crossing of retinal axons in the mouse visual system. Neuron 33:219–232

44. Erskine L, Williams S, Brose K, Kidd T, Rachel R, Goodman C, Tessier-Lavigne M, Mason C (2000) Retinal ganglion cell axon guidance in the mouse optic chiasm: expression and function of robos and slits. J Neurosci 20:4975–4982

45. Zolessi F, Poggi L, Wilkinson C, Chien C, Harris W (2006) Polarization and orientation of retinal ganglion cells in vivo. Neural Dev 1:1–21

46. Tosa Y, Tsukano K, Itoyama T, Fukagawa M, Nii Y, Ishikawa R, Suzuki KT, Fukui M, Kawaguchi M, Murakami Y (2015) Involvement of Slit-Robo signaling in the development of the posterior commissure and concomitant swimming behavior in *Xenopus laevis*. Zool Lett 1:28

47. Hofmeister W, Devine CA, Rothnagel JA, Key B (2012) Frizzled-3a and slit2 genetically interact to modulate midline axon crossing in the telencephalon. Mech Dev 129(5–8):109–124

48. Devine CA, Key B (2008) Robo-Slit interactions regulate longitudinal axon pathfinding in the embryonic vertebrate brain. Dev Biol 313(1):371–383

49. Philipp M, Niederkofler V, Debrunner M, Alther T, Kunz B, Stoeckli ET (2012) RabGDI controls axonal midline crossing by regulating Robo1 surface expression. Neural Dev 7:36

50. Brose K, Bland K, Wang K, Arnott D, Henzel W, Goodman C, Tessier-Lavigne M, Kidd T (1999) Slit proteins bind Robo receptors and have an evolutionarily conserved role in repulsive axon guidance. Cell 96:795–806

51. Chung WCJ, Moyle SS, Tsai PS (2008) Fibroblast growth factor 8 signaling through FGF receptor 1 is required for gonadotropin-releasing hormone neuronal development in mice. Endocrinology 149(10):4997–5003

52. Yamagishi M, Okamoto H (2010) Competition for ligands between FGFR1 and FGFR4 regulates *Xenopus* neural development. Int J Dev Biol 54:93–104

53. Heller N, Brändli A (1992) *Xenopus* Pax-2/5/8 orthologues: novel insights into Pax gene evolution and identification of Pax-8 as the earliest marker for otic and pronephric cell lineages. Dev Genet 24:208–219

54. Choubey L, Collette JC, Smith KM (2017) Quantitative assessment of fibroblast growth factor receptor 1 expression in neurons and glia. PeerJ 5:e3173

55. Frinchi M, Bonomo A, Trovato-Salinaro A, Condorelli DF, Fuxe K, Spampinato MG, Mudo G (2008) Fibroblast growth factor-2

and its receptor expression in proliferating precursor cells of the subventricular zone in the adult rat brain. Neurosci Lett 447(1):20–25

56. Mehlen P, Delloye-Bourgeois C, Chédotal A (2011) Novel roles for Slits and netrins: axon guidance cues as anticancer targets? Nat Rev Cancer 11:188–197

57. Amodeo V, Deli A, Betts J, Bartesaghi S, Zhang Y, Richard-Londt A, Ellis M, Roshani R, Vouri M, Galavotti S, Oberndorfer S, Leite AP, Mackay A, Lampada A, Stratford E, Li N, Dinsdale D, Grimwade D, Jones C, Nicotera P, Michod D, Brandner S, Salomoni P (2017) A PML/Slit axis controls physiological cell migration and cancer invasion in the CNS. Cell Rep 20:411–426

58. Ballard MS, Hinck L (2012) A roundabout way to cancer. Adv Cancer Res 114:187–235

59. Zhou WJ, Geng ZH, Chi S, Zhang W, Niu XF, Lan SJ, Ma L, Yang X, Wang LJ, Ding YQ, Geng JG (2011) Slit-Robo signaling induces malignant transformation through Hakai-mediated E-cadherin degradation during colorectal epithelial cell carcinogenesis. Cell Res 21(4):609–626

60. Yang XM, Han HX, Sui F, Dai YM, Chen M, Geng JG (2010) Slit-Robo signaling mediates lymphangiogenesis and promotes tumor lymphatic metastasis. Biochem Biophys Res Commun 396(2):571–577

61. Zhang B, Dietrich UM, Geng JG, Bicknell R, Esko JD, Wang L (2009) Repulsive axon guidance molecule Slit3 is a novel angiogenic factor. Blood 114:4300–4309

62. Wang B, Xiao Y, Ding BB, Zhang N, Yuan XB, Gui L, Qian KX, Duan S, Chen Z, Rao Y, Geng JG (2003) Induction of tumor angiogenesis by Slit-Robo signaling and inhibition of cancer growth by blocking Robo activity. Cancer Cell 4(1):19–29

63. Kong R, Yi F, Wen P, Liu J, Chen X, Ren J, Li X, Shang Y, Nie Y, Wu K, Fan D, Zhu L, Feng W, Wu JY (2015) Myo9b is a key player in SLIT/ROBO-mediated lung tumor suppression. J Clin Invest 125(12):4407–4420

64. Dunwell TL, Dickinson RE, Stankovic T, Dallol A, Weston V, Austen D, Catchpoole D, Maher ER, Latif F (2009) Frequent epigenetic inactivation of the SLIT2 gene in chronic and acute lymphocytic leukemia. Epigenetics 4(4):265–269

65. Huang P, Kishida S, Cao D, Murakami-Tonami Y, Mu P (2011) The neuronal differentiation factor NeuroD1 downregulates the neuronal repellent factor Slit2 expression and promotes cell motility and tumor formation of neuroblastoma. Cancer Res 71(8):2938–2948

66. Vaughen J, Igaki T (2016) Slit-Robo repulsive signaling extrudes tumorigenic cells from epithelia. Dev Cell 39:683–695

67. Jacobi A, Schmalz A, Bareyre FM (2014) Abundant expression of guidance and synaptogenic molecules in the injured spinal cord. PLoS One 9(2):e88449

68. Giger RJ, Hollis ER, Tuszynski MH (2010) Guidance molecules in axon regeneration. Cold Spring Harb Perspect Biol 2(7):a001867